Spin-dominated oxygen activation and reduction mechanism on Ru-N-C single-atom-catalyst

Zixian Zhao[1,2,3], Mingyuan Yu[1,2,3], Erjun Kan[1,2,3], Cheng Zhan[1,2,3]*
[1]School of Physics, Nanjing University of Science and Technology, Nanjing, Jiangsu Province, China 210094
[2]MIIT Key Laboratory of Semiconductor Microstructure and Quantum Sensing, Nanjing University of Science and Technology, Nanjing, Jiangsu Province, China 210094
[3]Engineering Research Center of Semiconductor Device Optoelectronic Hybrid Integration in Jiangsu Province, Nanjing, Jiangsu Province, China 210094
Email of corresponding author: czhan@njust.edu.cn

Gibbs free energy calculation at constant potential:

The four-step proton-coupled electron transfer process in ORR is defined as follows :

$$* + O_2 \rightarrow *OO \quad \text{(S1)}$$

$$*OO + H^+ + e^- \rightarrow *OOH \quad \text{(S2)}$$

$$*OOH + H^+ + e^- \rightarrow *O + H_2O \quad \text{(S3)}$$

$$*O + H_2O + H^+ + e^- \rightarrow *OH + H_2O \quad \text{(S4)}$$

$$*OH + H_2O + H^+ + e^- \rightarrow * + 2H_2O \quad \textit{(S5)}$$

where * represent the catalytic site. At U = 0 V *vs.* SHE, the free energy of proton-electron pair was set as the chemical potential of $1/2H_2$,[1] and then its free energy at any potential U can be expressed as:

$$G_{H+}(U) + G_{e-}(U) = G_{H+}(U) - e*(4.6 + U) = \frac{1}{2}G_{H_2} - e*U \quad \text{(S6)}$$

and the G_{H2} can be calculated by:

$$G_{H_2} = E_{H_2} + E_{ZPE} - T*S \quad \text{(S7)}$$

The E_{H2} was calculated by DFT, E_{ZPE} is zero-point energy obtained from vibration calculation at T=298.15 K and P = 1 bars. *S* is standard entropy from thermodynamic table.

For liquid water calculations, we consider the chemical potential of liquidwater is equal to the chemical potential of water in the gas phase at T = 298.15 K and P = 0.035 bars. [2]

Since the energy of O_2 cannot be accurately calculated using DFT, we make the following approximation:

$$G_{O_2} = (2G_{H_2O} - 2G_{H_2} - 4.92eV) \tag{S8}$$

In addition, we also performed thermodynamic corrections on the adsorption state free energy:[3]

$$G(U) = E(U) + E_{ZPE} - T * S \tag{S9}$$

Finally, the reaction free energy of ORR can be expressed as:

$$\Delta G_1 = G_{*OO} - G_* - G_{O_2} \tag{S10}$$

$$\Delta G_2 = G_{*OOH} - G_{*OO} - \frac{1}{2}G_{H_2} + e * U \tag{S11}$$

$$\Delta G_3 = G_{*O} + G_{H_2O} - G_{*OOH} - \frac{1}{2}G_{H_2} + e * U \tag{S12}$$

$$\Delta G_4 = G_{*OH} - G_{*O} - \frac{1}{2}G_{H_2} + e * U \tag{S13}$$

$$\Delta G_5 = G_* + G_{H_2O} - G_{*OH} - \frac{1}{2}G_{H_2} + e * U \tag{S14}$$

Micro-kinetic method:

Inspired by previous study ,[4] we constructed a microkinetic model for the ORR process over Ru-N-C SACs. We assume that the reaction occurs with bare RuN_4 and RuN_4 with one coordination, and the reaction rate at the site is described by the reaction rate of the rate-limiting step. Therefore, the reaction rate can be written as:

$$R(U) = \sum k_i(U)[C_i(U)] \tag{S15}$$

where *R(U)* is the total reaction rate, $k_i(U)$ are the reaction rates in corresponding active sites. $C_i(U)$ is the concentration of various possible active sites.

Based on classical transition theory, the $k_i(U)$ can be calculated by:

$$k_i(U) = A_i exp(\frac{-E_{a,i}}{k_B T}) exp(\frac{-G_i^b(U)}{k_B T}) \tag{S16}$$

A_i , $E_{a,i}$ are effective pre-exponential factor and activation energy, which can be

estimated to be 0.26 eV and 1.23×109 s-1.[5, 6] k_B is Boltzmann constant. $G_i^b(U)$ is the reaction barrier. It should be noted that there is a limit to the reaction rate of ORR due to the solubility limit of oxygen.[7] The reaction rate changes to:

$$k_i(U) = exp(\frac{-E_{a,i}}{k_B T}) min\left(A_i exp\left(\frac{-G_i^b(U)}{k_B T}\right), v_{O_2}\right) \quad \text{(S17)}$$

The values of v_{O2} is taken as 1×10^8 s^{-1}.[8]

In addition, the concentration $C_i(U)$ is balanced according to total site concentration following the formula:

$$[M] = \sum [C_i(U)] \quad \text{(S18)}$$

where M is total concentration of active sites, which can be computed by active sites divided by surface area. Besides, $C_i(U)$ follow the equilibrium constants:

$$K_i(U) = \frac{C_i(U)}{C_0(U)} = exp\left(\frac{-G_i^f(U)}{kT}\right) \quad \text{(S19)}$$

$C_0(U)$ is concentration of RuN_4^{IS}, the $G_i^f(U)$ is formation energy of various active site relative to RuN_4^{IS}. The ρ_{Fe} in our simulation model is set to 2.10E+13 cm^{-2}, corresponding to the experimental loadings about 3% wt.[9]

Finally, the current density can be calculated as:

$$j(U) = \frac{nFR(U)}{N_A} \quad \text{(S20)}$$

Where n is the charge transfer of reaction, F is Faraday constant, and N_A is the Avogadro constant.

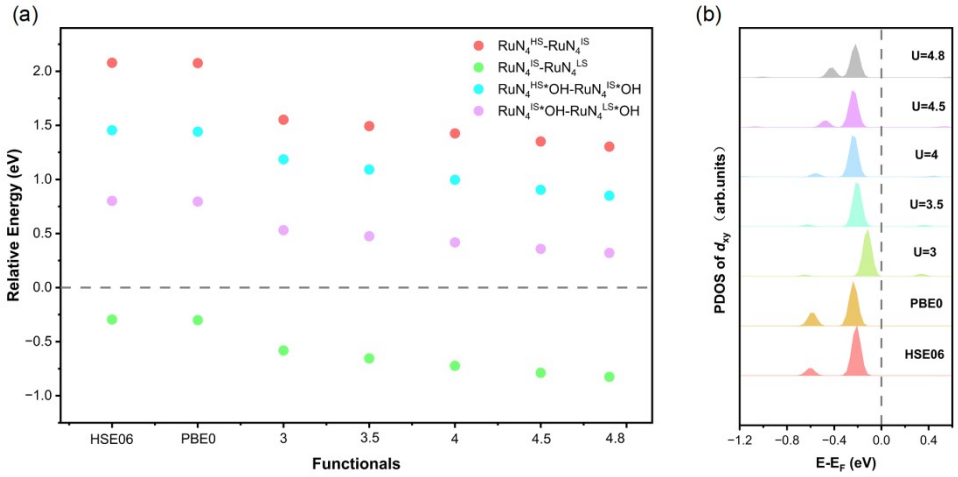

Figure S1. Relative energy of different spin states of RuN_4 and RuN_4*OH. (a) using different functionals and using DFT+U with different Ueff, (b)PDOS of Ru $4d_{xy}$ orbitals in RuN_4^{HS}.

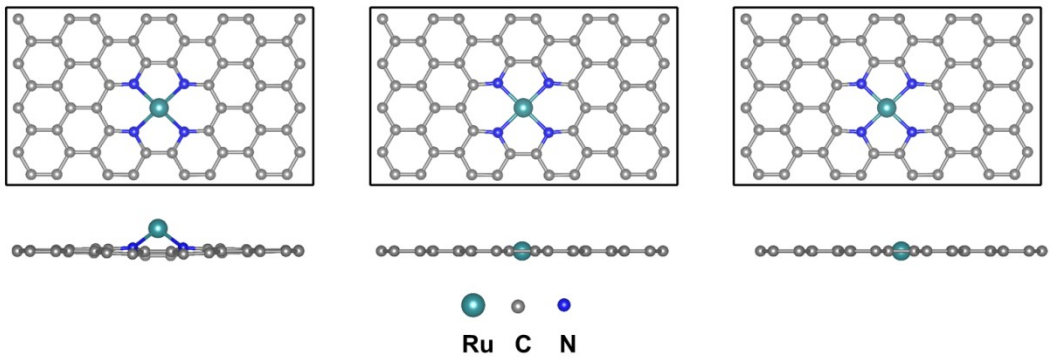

Figure S2. The RuN_4 models for different spin states. (a) RuN_4^{HS}, (b) RuN_4IS,(c) RuN_4^{LS}. The balls colored teal, gray, and blue represent Ru , C , and N atoms, respectively.

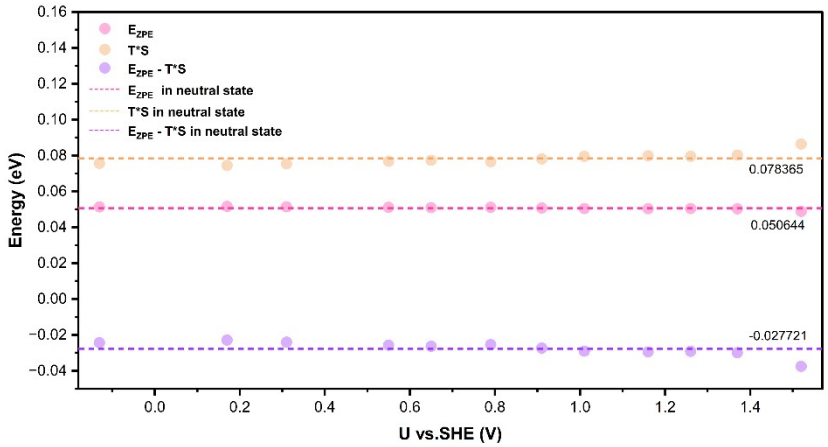

Figure S3. The effect of voltage on the zero-point energy (ZPE) and entropy term (TS) for RuN_4^{IS}.

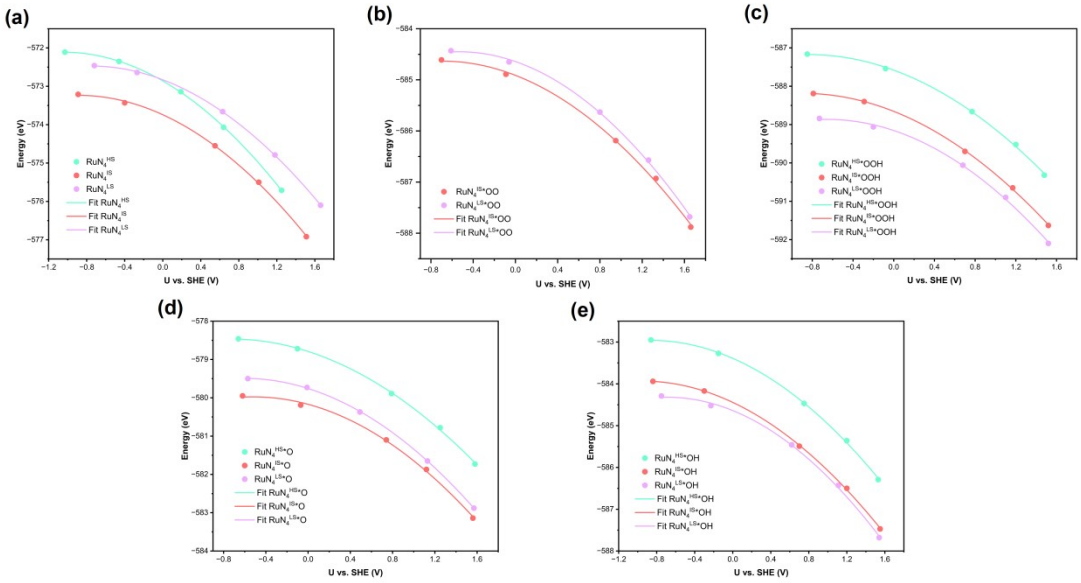

Figure S4. Free energy of high spin, intermediate spin and low spin state at different potential and fitted curves. (a) RuN_4, (b) RuN_4*OO, (c) RuN_4*OOH, (d) RuN_4*O, (e) RuN_4*OH.

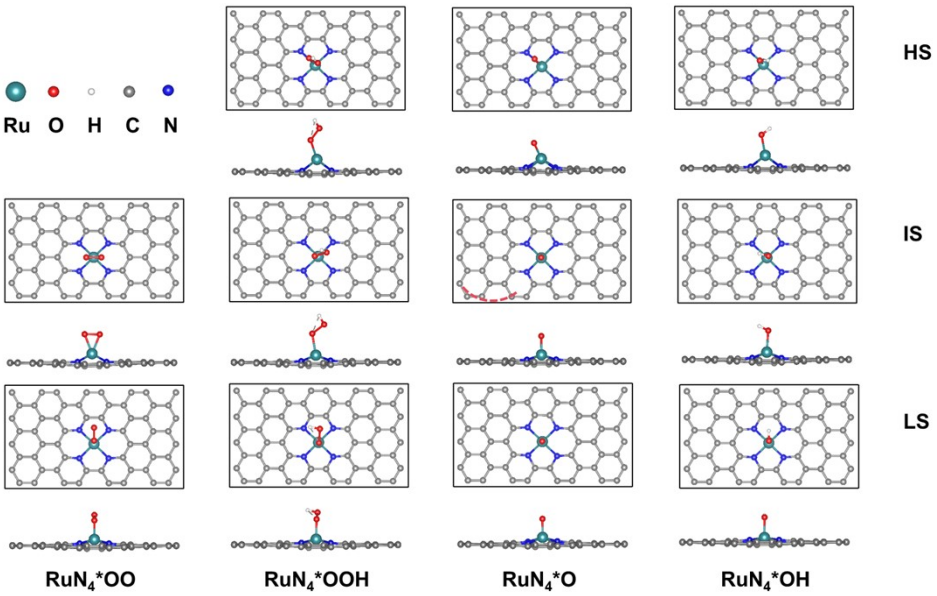

Figure S5. The RuN_4 intermediates models for different spin states. The balls colored teal, gray, and blue represent Ru, C, and N atoms, respectively.

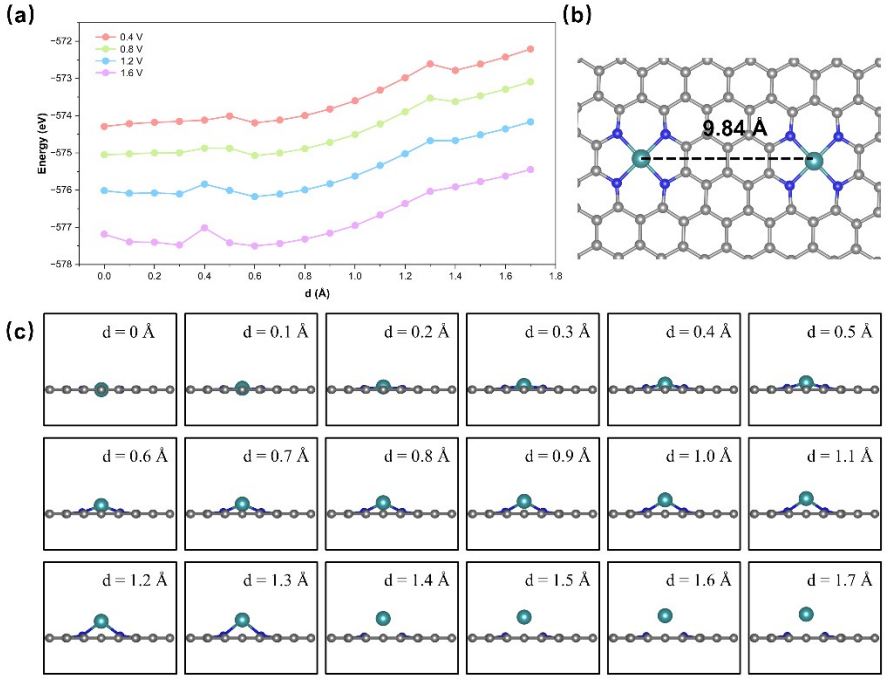

Figure S6. Ru out-of-plane displacement for (a) the energy variation and (b) the structure ;(c) RuN_4 structure and nearest distance .

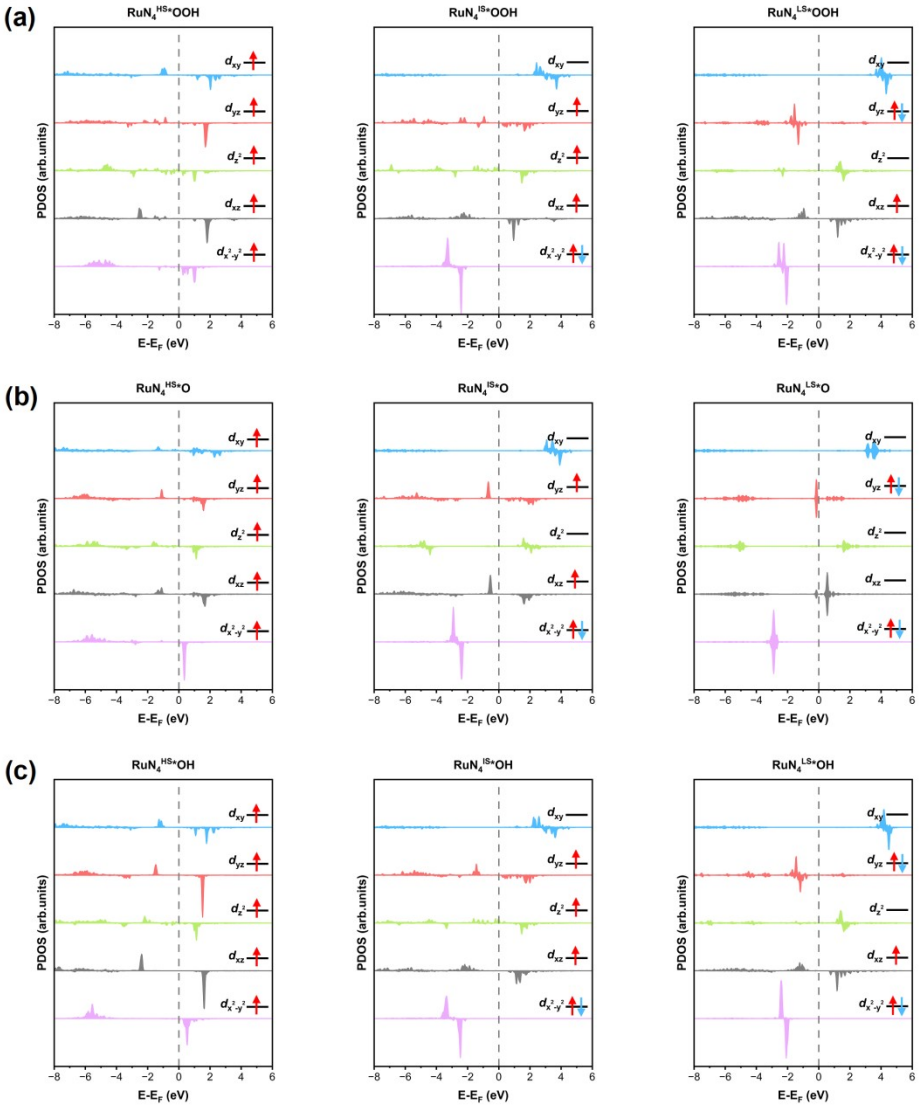

Figure S7. PDOS of Ru 4d orbitals, separated by spin-up and spin-down: (a) RuN_4*OOH, (b) RuN_4*OO, and (c) RuN_4*OH.

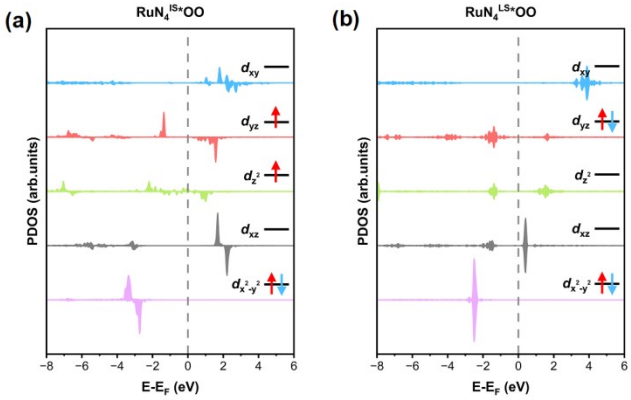

Figure S8. PDOS of Ru 4d orbitals, separated by spin-up and spin-down: (a) RuN_4^{IS}*OO, (b) RuN_4^{LS}*OO.

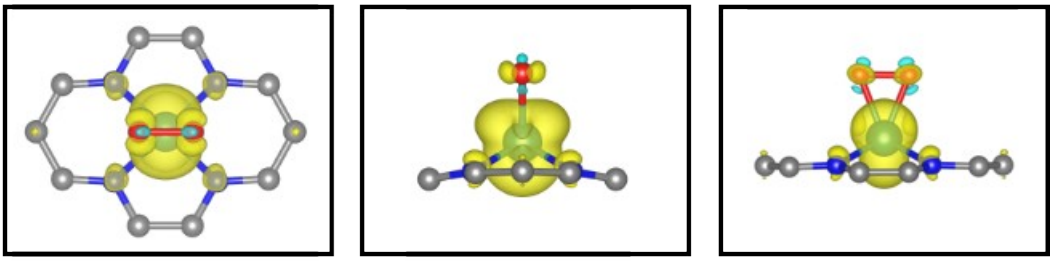

Figure S9. Spin density of RuN_4^{IS}. (Iso-surface: 0.004e/ bohr3)

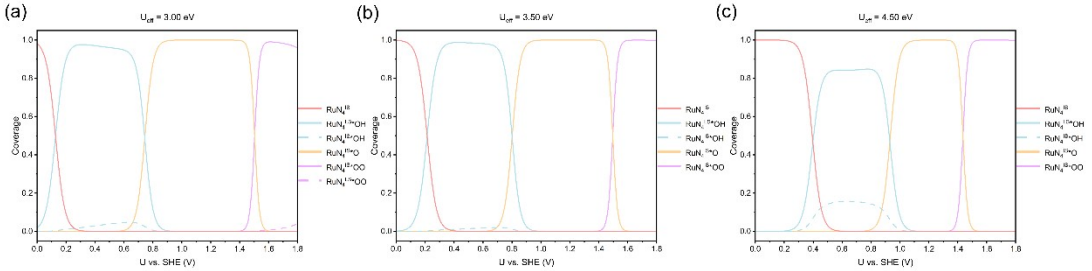

Figure S10. Coverages of active moieties vs. potential in (a) Ueff = 3.00 eV ;(b) Ueff = 3.50 eV ; (c) Ueff = 3.00 eV.

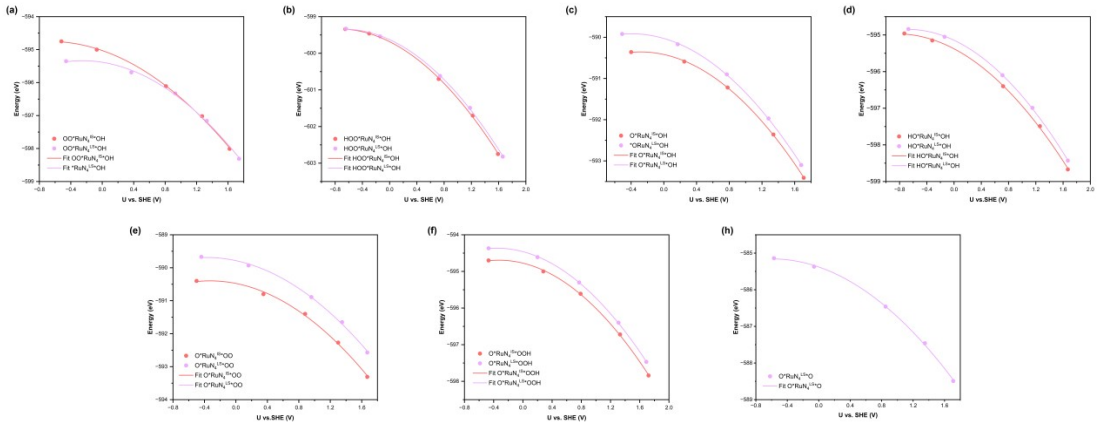

Figure S11. Free energy of intermediate spin and low spin at different potential and fit curves. (a)HO*RuN_4*OO, (b) HO*RuN_4*OOH, (c) HO*RuN_4*O, (d) HO*RuN_4*OH, (e) O*RuN_4*OO, (f)O*RuN_4*OOH, (h) O*RuN_4*OH.

Table S1. Total energy and structural parameters of RuN_4 and its ORR intermediates in neutral state.

	E	Ru-N(Å)	dRu(Å)
RuN_4^{IS}*OO	-584.80	2.07	0.78
RuN_4^{LS}*OO	-584.69	1.99	0.45
RuN_4^{HS}*OOH	-587.35	2.21	1.08
RuN_4^{IS}*OOH	-588.42	2.02	0.56
RuN_4^{LS}*OOH	-589.10	1.99	0.37
RuN_4^{HS}*O	-578.67	2.15	0.95
RuN_4^{IS}*O	-580.20	2.00	0.47
RuN_4^{LS}*O	-579.74	1.98	0.49

RuN_4^{HS}*OH	-583.16	2.21	1.09
RuN_4^{IS}*OH	-584.16	2.21	0.59
RuN_4^{LS}*OH	-584.56	1.98	0.32

Table S2. 4d orbital occupations for Ru ion in different structures.

Ru spin states	Majority spin					Minority spin				
	d_{xy}	d_{yz}	d_{z2}	d_{xz}	d_{x2-y2}	d_{xy}	d_{yz}	d_{z2}	d_{xz}	d_{x2-y2}
					RuN_4					
HS	0.877	0.917	0.909	0.918	0.892	0.183	0.126	0.124	0.101	0.872
IS	0.437	0.824	0.840	0.886	0.896	0.398	0.763	0.098	0.088	0.883
LS	0.426	0.727	0.796	0.236	0.890	0.426	0.726	0.796	0.233	0.890
					RuN_4*OO					
IS	0.414	0.924	0.873	0.491	0.895	0.361	0.211	0.428	0.423	0.888
LS	0.406	0.768	0.534	0.460	0.891	0.406	0.768	0.534	0.463	0.891
					RuN_4*OOH					
HS	0.923	0.921	0.903	0.916	0.910	0.247	0.221	0.397	0.154	0.121
IS	0.427	0.890	0.858	0.896	0.897	0.363	0.244	0.317	0.140	0.884
LS	0.413	0.810	0.438	0.903	0.891	0.393	0.780	0.389	0.204	0.886
					RuN_4*O					
HS	0.758	0.840	0.872	0.838	0.913	0.330	0.345	0.422	0.311	0.160
IS	0.421	0.876	0.523	0.919	0.894	0.388	0.348	0.490	0.325	0.887
LS	0.423	0.731	0.525	0.465	0.894	0.423	0.732	0.525	0.465	0.894
					RuN_4*OH					
HS	0.932	0.933	0.902	0.929	0.911	0.261	0.219	0.358	0.134	0.067
IS	0.427	0.895	0.848	0.912	0.897	0.358	0.203	0.322	0.142	0.882
LS	0.422	0.810	0.429	0.900	0.890	0.399	0.780	0.383	0.189	0.887
					HO*RuN_4*OO					
IS	0.442	0.802	0.451	0.893	0.892	0.418	0.432	0.415	0.393	0.886
LS	0.424	0.823	0.428	0.835	0.893	0.406	0.795	0.395	0.191	0.889
					HO*RuN_4*OOH					
IS	0.455	0.884	0.448	0.896	0.895	0.423	0.290	0.424	0.410	0.887
LS	0.430	0.801	0.438	0.483	0.891	0.430	0.801	0.438	0.483	0.891
					HO*RuN_4*O					
IS	0.433	0.864	0.496	0.899	0.895	0.402	0.344	0.483	0.324	0.888
LS	0.438	0.780	0.507	0.385	0.897	0.438	0.779	0.507	0.385	0.897
					HO*RuN_4*OH					
IS	0.477	0.899	0.477	0.913	0.901	0.435	0.262	0.445	0.193	0.893

LS	0.430	0.811	0.440	0.451	0.893	0.430	0.811	0.440	0.451	0.893
					O*RuN$_4$*OO					
IS	0.434	0.867	0.519	0.883	0.895	0.403	0.358	0.491	0.335	0.888
LS	0.444	0.641	0.524	0.535	0.892	0.444	0.640	0.524	0.537	0.892
					O*RuN$_4$*OOH					
IS	0.433	0.859	0.501	0.896	0.895	0.402	0.355	0.485	0.331	0.887
LS	0.433	0.773	0.507	0.411	0.896	0.433	0.773	0.507	0.411	0.896
					O*RuN$_4$*O					
LS	0.473	0.547	0.584	0.481	0.902	0.473	0.547	0.584	0.481	0.902

Table S3. The free energy at neutral state E_0, potential of zero charge U_0 and fitted parameters of quadratic equation for calculating the total energies of various models.

model	C(e/V)	U_0(V/SHE)	E_0(eV)
RuN$_4^{HS}$	1.37	-1.05	-572.31
RuN$_4^{IS}$	1.27	-0.89	-573.34
RuN$_4^{LS}$	1.24	-0.76	-572.54
RuN$_4^{IS}$*OO	1.15	-0.69	-584.67
RuN$_4^{LS}$*OO	1.34	-0.53	-584.50
RuN$_4^{HS}$*OOH	1.15	-0.84	-587.23
RuN$_4^{IS}$*OOH	1.18	-0.89	-588.26
RuN$_4^{LS}$*OOH	1.35	-0.65	-588.94
RuN$_4^{HS}$*O	1.21	-0.73	-578.52
RuN$_4^{IS}$*O	1.45	-0.52	-580.04
RuN$_4^{LS}$*O	1.43	-0.61	-579.57
RuN$_4^{HS}$*OH	1.15	-0.86	-583.02
RuN$_4^{IS}$*OH	1.12	-0.95	-583.99
RuN$_4^{LS}$*OH	1.34	-0.69	-584.40
HO*RuN$_4^{IS}$*OH	1.17	-0.83	-595.03
HO*RuN$_4^{LS}$*OH	1.30	-0.68	-594.92
HO*RuN$_4^{IS}$*OOH	1.24	-0.75	-599.40
HO*RuN$_4^{LS}$*OOH	1.27	-0.67	-599.40
HO*RuN$_4^{IS}$*O	1.53	-0.29	-590.38
HO*RuN$_4^{LS}$*O	1.48	-0.39	-589.95
HO*RuN$_4^{IS}$*OO	1.23	-0.67	-594.80
HO*RuN$_4^{LS}$*OO	1.48	-0.25	-595.35
O*RuN$_4^{IS}$*OO	1.44	-0.33	-590.42
O*RuN$_4^{LS}$*OO	1.36	-0.38	-589.71
O*RuN$_4^{IS}$*OOH	1.50	-0.33	-594.72
O*RuN$_4^{LS}$*OOH	1.48	-0.36	-594.40
O*RuN$_4^{LS}$*O	1.24	-0.60	-585.20

Table S4. Total energy and structural parameters of RuN_4 ORR intermediates with dual side adsorbates in neutral state.

model	E	Ru-N(Å)	dRu(Å)
HO*RuN_4^{IS}*OH	-594.96	1.97	0.01
HO*RuN_4^{LS}*OH	-594.84	1.96	0.01
HO*RuN_4^{IS}*OOH	-599.34	1.97	0.03
HO*$RuN4^{LS}$*OOH	-599.33	1.97	-0.03
HO*RuN_4^{IS}*O	-590.36	1.98	-0.16
HO*RuN_4^{LS}*O	-589.92	1.97	-0.17
HO*RuN_4^{IS}*OO	-594.75	1.97	0.12
HO*RuN_4^{LS}*OO	-595.35	1.97	0.10
O*RuN_4^{IS}*OO	-590.40	1.99	0.30
O*RuN_4^{LS}*OO	-589.67	1.98	0.17
O*RuN_4^{IS}*OOH	-594.70	1.99	0.22
O*RuN_4^{LS}*OOH	-594.37	1.98	0.19
O*RuN_4^{LS}*O	-585.14	1.98	0.03

Reference:

1 J. K. Nørskov, J. Rossmeisl, A. Logadottir, L. Lindqvist, J. R. Kitchin, T. Bligaard and H. Jónsson, *Phys. Chem. B*, 2004, **108**, 17886-17892.

2 I. C. Man, H. Y. Su, F. Calle‐Vallejo, H. A. Hansen, J. I. Martínez, N. G. Inoglu, J. Kitchin, T. F. Jaramillo, J. K. Nørskov and J. Rossmeisl, *ChemCatChem*, 2011, **3**, 1159-1165.

3 M. Li, L. Zhang, Q. Xu, J. Niu and Z. Xia, *J. Catal*, 2014, **314**, 66-72.

4 Y. Ping, R. J. Nielsen and W. A. Goddard, III, *J.Am.Chem.Soc.*, 2017, **139**, 149-155.

5 Y. Wang, Y.-J. Tang and K. Zhou, *J.Am.Chem.Soc.*, 2019, **141**, 14115-14119.

6 D. T. Limmer, A. P. Willard, P. Madden and D. Chandler, *Proc. Natl. Acad. Sci*, 2013, **110**, 4200-4205.

7 Z. Huang and Q. Tang, *Phys. Chem. C*, 2022, **126**, 21606-21615.

8 H. A. Hansen, V. Viswanathan and J. K. Nørskov, *Phys. Chem. C*, 2014, **118**, 6706-6718.

9 J. Chen, M. Wang, L. Chen, K. Guo, B. Liu, K. Wang, N. Li, L. Bao and X. Lu, *Adv. Energy Sustainability Res.*, 2024, **5**, 2400010.